HNUE JOURNAL OF SCIENCE DOI: 10.18173/2354-1059.2022-0023
Natural Sciences 2022, Volume 67, Issue 2, pp. 65-75
This paper is available online at http://stdb.hnue.edu.vn

PREDICTING ELASTIC MODULUS OF THE BODY-CENTERED CUBIC METALLIC FILMS

Duong Dai Phuong
Military College of Tank Armor Officer

Abstract. The elastic modulus of the body-centered cubic (BCC) films is studied based on the moment method. For Fe, Ta, and W films a clear elastic modulus dependence of the thickness at ambient conditions and under temperatures up to 2000 K. The obtained results of the values of elastic modulus metallic films are smaller than the corresponding values of bulk material. Calculated results show the effects of temperature and thickness of elastic modulus for Fe, Ta, and W metallic films. On the other hand, when the thickness of thin films is about 60nm then the elastic modulus of the BCC films approaches the values of bulk material. Our results are compared with the other theoretical results and experimental values of bulk materials.

Keywords*:* metallic films, moment method, elastic modulus.

1. Introduction

To date, metallic thin films have received much attention in material sciences due to their novel applications in technology and industry [1, 2]. They exhibit different thermal, mechanical, electrical, and optical properties compared to those of bulk materials [3-5]. The knowledge about the elastic quantities of the metallic films as bulk modulus B_T, Young's modulus *Y*, and shear modulus *G* enable to determine the stability and reliability of manufactured materials.

Great efforts with experimental and theoretical studies have been made to estimate the elastic property of metallic and nonmetallic films. Using both nano- and micro-indentation methods, F. Seifried *et al.* [6] measured Young's modulus of Mo, Nb, and Ta thin films on various scales. The measured data of thin films showed good agreement with bulk data. Progressive scratch tests showed the important role of plastic deformation on the metallic thin films at larger normal forces. D. Bernoulli *et al.* [7] deposited Ta and TaNi thin films by the Direct current (DC) magnetron sputtering method. The effects of the underlying substrate and N_2/Ar ratio on hardness and phase of Ta and TaNi thin films were observed. Various methods such as X-ray diffraction [8], Brillouin scattering [9] were

Received May 11, 2022. Revised June 13, 2022. Accepted June 20, 2022.
Contact Duong Dai Phuong, e-mail address: vanha318@yahoo.com

also used to determine the elastic properties of nonmetallic films. Literature data showed a significant difference between the mechanical properties of metallic thin films and the values of bulk [10, 11]. The measured elastic modulus of Cu, Ag, and Al films were smaller than the values of bulk [10, 12]. However, the previous studies estimated the elastic properties of films at low temperatures, and the effects of thickness on the elastic properties have not been studied in detail.

In this paper, we study the elastic quantities of films (Fe, Ta, W) by the moment method [12, 13]. The effects of thickness and temperature and thickness on the elastic quantities of Fe, Ta, and are evaluated in detail. The mechanical quantities of Fe, Ta, and W thin films are calculated under temperatures up to 2000 K using the Lennard-Jones potential.

2. Content

2.1. Theory

2.1.1. Expressions of the displacement

One separates metallic films has the thickness b into n_l layers. These layers are as Figure 1.

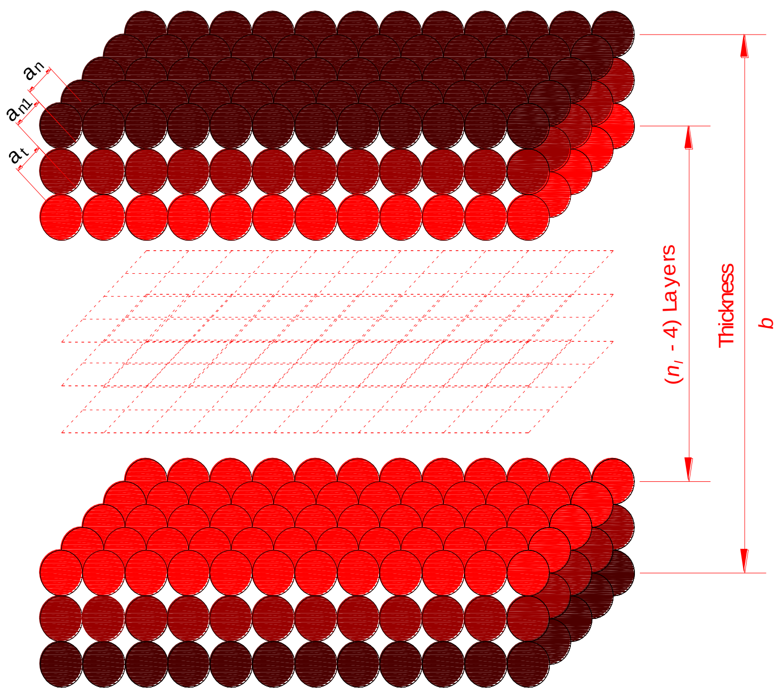

Figure 1. The metallic films

Equation of the displacement $<u_i^t>$ for internal layers atoms of metallic films [12, 13]

$$\gamma_t\theta^2 \frac{d^2 < u_i^t >}{dp^2} + 3\gamma_t\theta < u_i^t > \frac{d < u_i^t >}{dp} + \gamma_t < u_i^t >^3 + k_t < u_i^t > + \gamma_t \frac{\theta}{k_t}(x_t \coth x_t - 1) < u_i^t > - p = 0 , \tag{1}$$

where

$$x_t = \frac{\hbar\omega_t}{2\theta}; \theta = k_B T, k_t = \frac{1}{2}\sum_i \left(\frac{\partial^2 \varphi_{io}^t}{\partial u_{i\alpha}^2} \right)_{eq} \equiv m_0\omega_t^2, \tag{2}$$

$$\gamma_{1t} = \frac{1}{48}\sum_i \left(\frac{\partial^4 \varphi_{io}^t}{\partial u_{i\alpha}^4} \right)_{eq}, \gamma_{2t} = \frac{6}{48}\sum_i \left(\frac{\partial^4 \varphi_{io}^t}{\partial u_{i\beta}^2 \partial u_{i\gamma}^2} \right)_{eq}, \tag{3}$$

$$\gamma_t = \frac{1}{12}\sum_i \left[\left(\frac{\partial^4 \varphi_{io}^t}{\partial u_{i\alpha}^4} \right)_{eq} + 6\left(\frac{\partial^4 \varphi_{io}^t}{\partial u_{i\beta}^2 \partial u_{i\gamma}^2} \right)_{eq} \right] = 4\left(\gamma_{1t} + \gamma_{2t}\right), \tag{4}$$

with m_0 is the atomic mass of internal layers atoms, ω_t is the vibrational frequency of internal layers atoms; k_t, γ_{1t}, γ_{2t}, γ_t are the anharmonicity parameters; φ_{i0}^t is the effective interatomic potential.

The solution to equation (1) is as follows:

$$< u_i^t > = < u_i^t >_0 + A_1^t p + A_2^t p^2 \tag{5}$$

when the supplemental force p is at zero then the solution $< u_i^t >$ is given by

$$< u_i^t >_0 \approx \sqrt{\frac{2\gamma_t\theta^2}{3k_t^3} A_t}, \tag{6}$$

where

$$A_t = a_1^t + \frac{\gamma_t^2\theta^2}{k_t^4} a_2^t + \frac{\gamma_t^3\theta^3}{k_t^6} a_3^t + \frac{\gamma_t^4\theta^4}{k_t^8} a_4^t + \frac{\gamma_t^5\theta^5}{k_t^{10}} a_5^t + \frac{\gamma_t^6\theta^6}{k_t^{12}} a_6^t,$$

with the parameters $a_\eta^t (\eta = 1, 2..., 6)$ have the same forms as in Ref. [12, 13].

Similar to the internal layer atoms, the displacement of the next surface layers atoms is the solution of the equation as follows:

$$\gamma_1\theta^2 \frac{d^2 < u_i^{n1} >}{dp^2} + 3\gamma_{n1}\theta < u_i^{n1} > \frac{d < u_i^{n1} >}{dp} + \gamma_{n1} < u_i^{n1} >^3 + k_{n1} < u_i^{n1} > + \gamma_{n1} \frac{\theta}{k_{n1}}(x_{n1} \coth x_{n1} - 1) < u_i^{n1} > - p = 0 \tag{7}$$

The displacement of the surface layers atoms $< u_i^n >$ can be calculated by moment method formulation as follows:

$$k_n < u_i^n >_p + \gamma_n \left[< u_i^n >_p^2 + \theta \frac{\partial \left\langle u_i^n \right\rangle_p}{\partial p} + \frac{\theta}{m\omega_n^2} (x_n \coth x_n - 1) \right] - p = 0, \tag{8}$$

where

$$x_n = \frac{\hbar \omega_n}{2\theta}, \theta = k_B T \tag{9}$$

$$k_n = \frac{3}{2} \sum_i \left[\left(0^2 \varphi_{i0}^n \right) a_{ix}^2 + \left(0 \varphi_{i0}^n \right) \right] = m\omega_n^2, \tag{10}$$

$$\gamma_n = \sum_{\substack{i,\alpha,\beta,\gamma \\ \alpha \neq \beta}} \left[\frac{1}{4} \left(\frac{\partial^3 \varphi_{io}^n}{\partial u_{i\alpha,n}^3} \right)_{eq} + \frac{1}{4} \left(\frac{\partial^3 \varphi_{io}^n}{\partial u_{i\alpha,n}^2 \partial u_{i\gamma}^n} \right)_{eq} \right]. \tag{11}$$

when the supplemental force p is at zero then the solution $< u_i^t >$ is given by

$$< u_i^n > = < u_i^n >_0 + A_1^n p + A_2^n p^2. \tag{12}$$

here, $< u_i^n >_0$ can be calculated by moment method formulation. The expression of $< u_i^n >_0$ is given by

$$< u_i^n >_0 = -\frac{\gamma_n \theta}{k_n^2} x_n \coth x_n. \tag{13}$$

2.1.2. The expression of average displacement and free energy

The Helmholtz free energies of the internal layers and next surface layers are given by Ref. [12].

$$\Psi_t = \left\{ U_0^t + 3N_t\theta \left[x_t + ln\left(1 - e^{-2x_t}\right) \right] \right\} + \frac{3N_t\theta^2}{k_t^2} \left\{ \gamma_{2t} X_t^2 - \frac{2\gamma_{1t}}{3} \left(1 + \frac{X_t}{2} \right) \right\} + \frac{6N_t\theta^3}{k_t^4} \left\{ \frac{4}{3} \gamma_{2t}^2 \left(1 + \frac{X_t}{2} \right) X_t - 2\left(\gamma_{1t}^2 + 2\gamma_{1t}\gamma_{2t} \right) \left(1 + \frac{X_t}{2} \right) \left(1 + X_t \right) \right\}. \tag{14}$$

$$\Psi_{n1} = \left\{ U_0^{n1} + 3N_{n1}\theta \left[x_{n1} + ln\left(1 - e^{-2x_{n1}}\right) \right] \right\} + \frac{3N_{n1}\theta^2}{k_{n1}^2} \left\{ \gamma_{2n1} X_{n1}^2 - \frac{2\gamma_{1n1}}{3} \left(1 + \frac{X_{n1}}{2} \right) \right\} + \frac{6N_{n1}\theta^3}{k_{n1}^4} \left\{ \frac{4}{3} \gamma_{2n1}^2 \left(1 + \frac{X_{n1}}{2} \right) X_{n1} - 2\left(\gamma_{1n1}^2 + 2\gamma_{1n1}\gamma_{2n1} \right) \left(1 + \frac{X_{n1}}{2} \right) \left(1 + X_{n1} \right) \right\}. \tag{15}$$

with $X_t = x_t coth x_t$, $X_{n1} = x_{n1} coth x_{n1}$, and

$$U_0^t = \frac{N_t}{2} \sum \varphi_{i0}^t \left(r_{i,t} \right), U_0^{n1} = \frac{N_{n1}}{2} \sum \varphi_{i0}^{n1} \left(r_{i,n1} \right), \tag{16}$$

In the harmonic approximation, the Helmholtz free energy of the surface layers is determined as [13]

$$\Psi_n = \left\{ U_0^n + 3N_n\theta \left[x_n + ln\left(1 - e^{-2x_n}\right) \right] \right\} \tag{17}$$

One considers the system consisting of N_l atoms and the number of atoms in each layer is N_l , then

$$N = n_l N_l \ \Rightarrow n_l = \frac{N}{N_l}. \tag{18}$$

The numbers of atoms in the internal, next surface, and surface layers are determined as follows, respectively

$$N_t = \left(n_l - 4\right) N_l = \left(\frac{N}{N_l} - 4\right) N_l = N - 4N_l , \tag{19}$$

$$N_{n1} = 2N_l = N - (n_l - 2)N_l \text{ and } N_n = 2N_l = N - (n_l - 2)N_l. \tag{20}$$

The Helmholtz free energies of the system and an atom, respectively, are given by

$$\Psi = N_t \Psi_t + N_{n1} \Psi_{n1} + N_n \Psi_n = \left(N - 4N_l\right)\Psi_t + 2N_l \Psi_{n1} + 2N_l \Psi_n \tag{21}$$

$$\frac{\Psi}{N} = \left[1 - \frac{4}{n_l}\right]\Psi_t + \frac{2}{n_l}\Psi_{n1} + \frac{2}{n_l}\Psi_n \tag{22}$$

The average nearest-neighbor distance (NND) is denoted as a_{tb} and b_{tb} is the average two-layers thickness, then we have

$$b_{tb} = \frac{a_{tb}}{\sqrt{3}} . \tag{23}$$

On the other hand, the thickness b can be calculations

$$b = 2b_n + 2b_{n1} + \left(n_l - 5\right) b_t = \left(n_l - 1\right) b_{tb} = \left(n_l - 1\right) \frac{a_{tb}}{\sqrt{3}}. \tag{24}$$

From Eq. (24), we have

$$n_l = 1 + \frac{d}{b_{tb}} = 1 + \frac{d\sqrt{3}}{a_{tb}}. \tag{25}$$

The average nearest-neighbor distance is given by

$$a_{tb} = \frac{2a_n + 2a_{n1} + (n_l - 5)a_t}{n_l - 1}. \tag{26}$$

In Eq. (25), a_n , a_{n1} and a_t have the from

$$a_n = a_{0,n} + < u_i^n >_0 , a_{n1} = a_{0,n1} + < u_i^{n1} >_0 , a_t = a_{0,t} + < u_i^t >_0 , \tag{27}$$

From Eqs. (22) and (25), Substituting Eq. (24) into Eq. (23), we determined the expression of the Helmholtz free energy

$$\frac{\Psi}{N} = \frac{b\sqrt{3} - 3a_{tb}}{b\sqrt{3} + a_{tb}} \Psi_t + \frac{2a_{tb}}{b\sqrt{3} + a_{tb}} \Psi_n + \frac{2a_{tb}}{b\sqrt{3} + a_{tb}} \Psi_{n1} \tag{28}$$

2.1.3. The elastic quantities of the BCC metallic films

The elastic quantities of metallic films are derived based on thermodynamic relations. The bulk modulus B_T is determined

$$B_T = -V_0\left(\frac{\partial P}{\partial V}\right)_T$$
$$= \left(\frac{a_{0tb}}{a_{tb}}\right)^3\left[\frac{2}{3}P + \frac{a_{tb}^2}{9V}\left(\frac{b\sqrt{3}-3a_{tb}}{b\sqrt{3}+a_{tb}}\frac{\partial^2\Psi_t}{\partial a_t^2} + \frac{2a_{tb}}{b\sqrt{3}+a_{tb}}\frac{\partial^2\Psi_n}{\partial a_n^2} + \frac{2a_{tb}}{b\sqrt{3}+a_{tb}}\frac{\partial^2\Psi_{n1}}{\partial a_{n1}^2}\right)_T\right] \tag{29}$$

The Helmholtz free energy for surface layers atoms $\psi_{p,n}$ is given by

$$\Psi_{p,n} = \Psi_{0,n} + \frac{\sigma_n\varepsilon_n}{2} = \Psi_{0,n} + \frac{Y_n\varepsilon_n^2}{2}, \tag{30}$$

with ε_n is the elastic strain, $\sigma_n = Y_n\varepsilon_n$ is the stress.

From Eq. (30), one derives

$$\frac{\partial\Psi_{p,n}}{\partial\varepsilon_n} = \frac{\partial\Psi_{p,n}}{\partial\sigma_n}\frac{\partial\sigma_n}{\partial\varepsilon_n} = Y_n\varepsilon_n. \tag{31}$$

Another face, in the elastic deformation then we have

$$\varepsilon_n = \frac{\Delta a_n}{a_n} = \frac{a_{p,n}-a_n}{a_n}, \tag{32}$$

where a_n and $a_{p,n}$ can be given by

$$\left.\begin{aligned} a_n &= a_{0,n} + y_0^n \\ a_{p,n} &= a_{0p,n} + y_n \end{aligned}\right\}. \tag{33}$$

On the other hand, from a relationship

$$p = \sigma_n S_n = \sigma_n \pi a_n^2. \tag{34}$$

when p is small then we have

$$\varepsilon_n = \frac{a_{p,n}-a_n}{a_n} \approx \frac{y_n - y_0^n}{a_n} \approx \frac{A_1^n p}{a_n}, \tag{35}$$

where, A_1^n has form as [12, 13]:

$$A_1^n = \frac{1}{k_n}\left[1 + \frac{2\gamma_n^2\theta^2}{k_n^4}\left(1 + \frac{x_n\coth x_n}{2}\right)\left(1 + x_n\coth x_n\right)\right]. \tag{36}$$

From Eqs. (34), (35), (36), and (31), for surface layers atoms of metallic thin film, expression of Young's modulus is given by

$$Y_n = \frac{\sigma_n a_n}{A_1^n p} = \frac{1}{\pi a_n A_1^n} = \frac{1}{\pi\left(a_{0,n} + y_0^n\right)A_1^n}. \tag{37}$$

Similar to the next surface layers atoms and internal layers, we can be determined

$$Y_{n1} = \frac{\sigma_{n1} a_{n1}}{A_1^{n1} p} = \frac{1}{\pi a_{n1} A_1^{n1}} = \frac{1}{\pi \left(a_{0,n1} + y_0^{n1} \right) A_1^{n1}}, \tag{38}$$

$$Y_t = \frac{\sigma_t a_t}{A_1^t p} = \frac{1}{\pi a_t A_1^t} = \frac{1}{\pi \left(a_{0,t} + y_0^t \right) A_1^t}, \tag{39}$$

where A_1^{n1} and A_1^t have formed as

$$A_1^{n1} = \frac{1}{k_{n1}} \left[1 + \frac{2\gamma_{n1}^2 \theta^2}{k_{n1}^4} \left(1 + \frac{x_{n1} \coth x_{n1}}{2} \right) \left(1 + x_{n1} \coth x_{n1} \right) \right] \tag{40}$$

$$A_1^t = \frac{1}{k_t} \left[1 + \frac{2\gamma_t^2 \theta^2}{k_t^4} \left(1 + \frac{x_t \coth x_t}{2} \right) \left(1 + x_t \coth x_t \right) \right]. \tag{41}$$

The Young's modulus and shear modulus of metallic films with body-centered cubic structure is given respectively

$$Y = \frac{2Y_n + 2Y_{n1} + \left(n_l - 5 \right) Y_t}{n_l - 1}. \tag{42}$$

$$G = \frac{Y}{2\left(1 + \upsilon \right)}. \tag{43}$$

In Eq. (25), the Poisson's ratio determined as

$$\upsilon = \frac{1}{2} \left(1 - \frac{Y}{3B_T} \right). \tag{44}$$

2.2. Numerical results and discussion

To calculate the elastic quantities of Fe, Ta, and W films, one uses the expressions derived in the previous section and the using the Lennard-Jones potential [14]

$$\varphi(r) = \frac{D}{(n-m)} \left[m \left(\frac{r_0}{r} \right)^n - n \left(\frac{r_0}{r} \right)^m \right], \tag{45}$$

In Eq. (45), the values of potential parameters for Fe, Ta, and W films are presented in Table 1.

Table 1. Lennard-Jones potential parameters of Fe, Ta, and W metallic thin films [14]

Metals	***n***	***m***	$r_0(\mathrm{A}^0)$	$D / k_B(\mathrm{K})$
Fe	8.26	3.58	2.4775	12576.70
Ta	11.16	2.52	2.8648	21305.51
W	8.58	4.06	2.7365	25608.93

From Eq. (26), we obtain the average NND of BCC metallic thin films. Based on the expressions obtained in Section 2, the elastic quantities including the analytic expressions for bulk modulus (B_T), Young's modulus (Y), and shear modulus (G) for Fe, Ta, and W films are calculated as functions of temperatures and thickness.

Figure 2 shows the temperature dependence of bulk modulus of Fe thin films. The bulk modulus with the various number of layers is presented as a function of temperature. One can see that when the temperature increases the bulk modulus decreases. The bulk modulus increases when the thickness of the thin film increases and approaches the value of bulk material [15]. Furthermore, at room temperature, the bulk modulus of the thin film is smaller than that of the bulk material. Our results are in accordance with the values presented in Ref. [15] for Fe bulk material. when the thickness of thin films is about 60nm then the bulk modulus of the thin film approaches the values of bulk material.

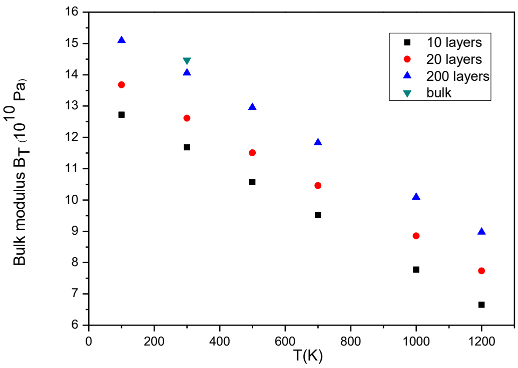

Figure 2. Temperature dependence of bulk modulus of Fe thin films

Figure 3 shows the temperature dependence of the shear modulus of Fe thin films. The shear modulus with the various number of layers is presented as a function of temperature. One can see that the shear modulus decrease with increasing temperature. With increasing thickness *b* then shear modulus *G* increases and approaches the value of bulk material at a number of 300 layers. Our results depend on the thickness and temperature of elastic quantities for Fe, Ta, and W films in accordance with the values presented in Ref. [16, 17].

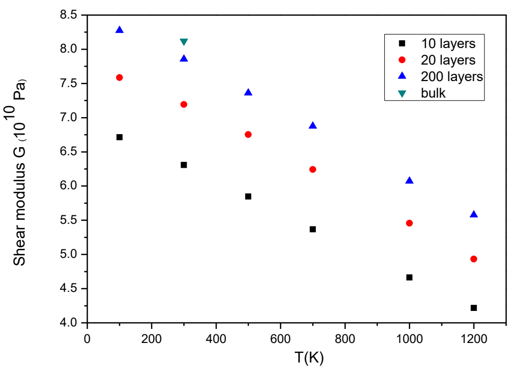

Figure 3. Temperature dependence of shear modulus of Fe thin film

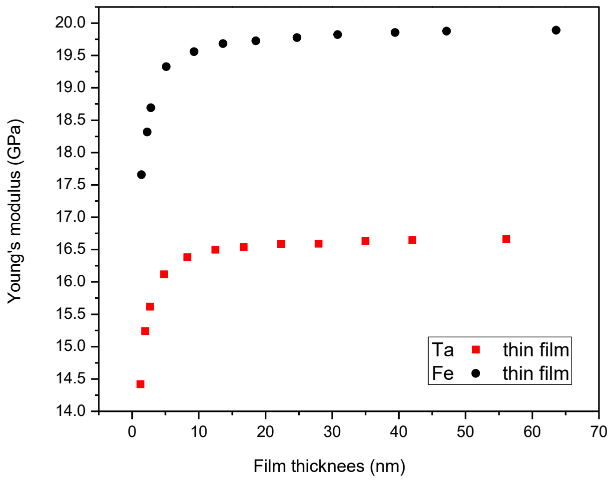

Figure 4. Thickness dependence of Young's modulus of Ta and Fe thin films

Table 2. Temperature dependence of elastic modulus of Ta thin films

Quantities	n_l **T (K)**		**100**	**300**	**500**	**700**	**1000**	**1200**
$B_T (10^{10}$ Pa)	SMM	10	15.8302	14.9387	14.0871	12.4157	10.7137	7.7427
		20	16.8630	15.9891	15.1557	13.5298	11.8916	9.1298
		200	17.9151	17.0691	16.2663	14.7185	13.1976	10.8854
		bulk	---	18.18	---	---	---	---
$Y (10^{10}$ Pa)	SMM	10	15.2322	14.4170	13.4771	11.2525	8.6672	4.6044
		20	16.4132	15.6151	14.7012	12.5499	10.0303	5.9276
		200	17.3746	16.5905	15.6976	13.6061	11.1400	7.0048
		bulk	---	17.45	---	---	---	---
	Ex. [15]	bulk	---	17.62	---	---	---	---
$G (10^{10}$ Pa)	SMM	10	5.5245	5.4123	5.2476	5.1437	4.8758	4.7169
		20	5.7856	5.6832	5.5114	5.3006	5.1320	4.9585
		200	6.2453	6.2213	6.0118	5.8612	5.5655	5.2579
		bulk	---	6.51	---	---	---	---
	Ex. [15]	bulk	---	6.52	---	---	---	---

Figure 4 displays the thickness dependence of the elastic modulus of Ta and Fe films at room temperature. The calculated values of elastic modulus are substantially lower than the bulk values. One can see that Young's modulus increases when the thickness of thin film increases and approaches the values of bulk material at a thickness of 60 nm [15]. On the other hand, when the thickness is larger than 60 nm then the elastic modulus for Fe, Ta, and W films less depends on the thickness. Furthermore, calculated results show Young's modulus in accordance with the law presented by X. Zhou *et al.* [16] and [17].

Similarly, the calculated results of elastic quantities for Ta and W metallic films are in Table 2 and Table 3. The mechanical quantities have a clear dependence on the thickness and temperature of metallic films.

Table 3. Temperature dependence of elastic modulus of W thin films

Quantities	T(K) / n_l		**200**	**300**	**500**	**800**	**1500**	**2000**
B_T (10^{10} Pa)	SMM	10	21.9515	21.4528	20.4374	18.9188	15.4582	13.0619
		20	27.5565	27.0515	26.0523	24.5748	21.2078	18.862
		200	29.5883	29.0825	28.0965	26.6478	23.3495	21.0462
		bulk	---	31.36	---	---	---	---
	Ex. [15]	bulk	---	30.00	---	---	---	---
Y(10^{10} Pa)	SMM	10	34.8352	34.5856	34.0717	33.2747	31.2992	29.7831
		20	36.6436	36.3723	35.8084	34.9345	32.7923	31.1713
		200	40.6337	40.3024	39.6002	38.5144	35.9123	34.002
		bulk	---	41.40	---	---	---	---
	Ex. [15]	bulk	---	41.50	---	---	---	---
G(10^{10} Pa)	SMM	10	13.0149	12.9279	12.7476	12.4663	11.7628	11.2179
		20	13.7870	13.6919	13.4931	13.1833	12.4176	11.8330
		200	14.9745	14.8566	14.6053	14.2150	13.2731	12.5764
		bulk	---	16.17	---	---	---	---
	Ex. [15]	bulk	---	16.00	---	---	---	---

3. Conclusions

The elastic modulus is performed based on the Lennard-Jones potential for Fe, Ta, and W of BCC metallic films. According to this study, the elastic modulus of BCC metallic films is predicted and the elastic modulus increases with increasing thickness. The bulk modulus B_T, Young's modulus *Y*, and shear modulus *G* of metallic thin films decrease with the increase in temperature. While they increase as the thickness for metallic films increases and approach the values of bulk materials with the thickness of 60 nm. Numerical calculations are performed for Fe, Ta, and W thin films. The calculated elastic modulus results are in accordance with the laws presented by the other theoretical and experimental results of bulk materials.

REFERENCES

[1] Hoo-Jeong Lee, 2004. Study on the strength and elongation of free-standing Al beams for microelectromechanical systems applications. *Appl. Phys. Lett.*, **84**, p. 915.

[2] Nobutomo Nakamura, Hirotsugu Ogi, and Masahiko Hirao, 2005. Elastic constants and magnetic anisotropy of Co⁄PtCo⁄Pt superlattice thin films. *Appl. Phys. Lett.*, **86,** 111918.

[3] H. Haibo, F. Spaepen, 2000. Tensile testing of free-standing Cu, Ag, and Al thin films and Ag/Cu multilayers. *Acta mater.*, **48**, pp. 3261-3269.

[4] Z. Yan-Feng, Z. Tang, H. Tie-Zhu, M. Xu-Cun, J. Jin-Feng, X. Qui-Kun, Kun Xun and W. Si-Cheng, 2007. Oscillatory thermal expansion of Pb thin films modulated by quantum size effects. *Applied physics letters*, **90**, 093120.

[5] S. Chen, L. Liu, T. Wang, 2005. Investigation of the mechanical properties of thin films by nanoindentation considering the effects of thickness and different coating-substrate combinations. *Surface & Coatings Technology,* **191**, pp. 25-32.

[6] F. Seifried, H. Leiste, R. Schwaiger, S. Ulrich, H.J. Seifert, M. Stueber, 2018. Structure, morphology and selected mechanical properties of magnetron sputtered (Mo, Ta, Nb) thin films on NiTi shape memory alloys. *Surface & Coatings Technology*, **347**, pp. 379-389.

[7] D. Bernoulli, U. Muller, M. Schwarzenberger, R. Hauert, R. Spolenak, 2013. Magnetron sputter deposited tantalum and tantalum nitride thin films: An analysis of phase, hardness and composition. *Thin Solid Films*, **548**, pp. 157-161.

[8] F.C. Marques, P. Wickboldt, D. Pang, J.H. Chen, W. Paul, 1998. Stress and thermomechanical properties of amorphous hydrogenated germanium thin films deposited by glow discharge. *J. Appl. Phys*., **84**, 3118.

[9] R. Bhadra, J. Pearson, P. Okamoto, L. Rehn, M. Grimsditch, 1988. Elastic properties of Si during amorphization. *Phys. Rev. B,* **38**, 12656.

[10] M.M. de Lima, R.G. Lacerda, J. Vilcarromero, F.C. Marques, 1999. Coefficient of thermal expansion and elastic modulus of thin films. *J. Appl. Phys*., **86**, 4936.

[11] A.J. Kalkman, A.H. Verbruggen, G.C.A.M. Janssen, 2001. Youngs modulus measurements and grain boundary sliding in free standing thin metal films. *Appl. Phys. Lett*., **78**, 2673.

[12] K. Masuda-Jindo, V.V. Hung, P.D. Tam, 2003. Thermodynamic quantities of metals are investigated by an analytic statistical moment method. *Phys. Rev. B,* **67**, 094301.

[13] N. Tang, V.V. Hung, 1988. Investigation of the thermodynamic properties of anharmonic crystals by the momentum method. I. General results for face-centred cubic crystals. *Phys. Stat. Sol. B,* **149**, 511.

[14] M. Magomedov, 2006. The calculation of the parameters of the mie-lennard-jones potential. *High Temperature,* **44** (4), pp. 513-529.

[15] B. H. Billings, et al., 1963. *American Institute of Physics Handbook.* McGraw-Hill Book Company, New York.

[16] X. Zhou, H. Ren, Y Zhang, T. Zhang, 2014. Size-dependent elastic properties of thin films: surface anisotropy and surface bonding. *Science China Tech. Sci.,* **57**, 680.

[17] Duong Dai Phuong, Nguyen Thi Hoa, Vu Van Hung, Doan Quoc Khoa and Ho Khac Hieu, 2016. Mechanical properties of metallic thin films: theoretical approach. *The European Phys. Journal B.,* **89** (3), DOI:10.1140/epjb/e2016-60583-y.